9770 *Inorg. Chem.* **2010**, *49*, 9770–9776
DOI: 10.1021/ic1004566

Inorganic Chemistry
Article

$9Mg(OH)_2 \cdot MgCl_2 \cdot 4H_2O$, a High Temperature Phase of the Magnesia Binder System

Robert E. Dinnebier,*,† Daniela Freyer,*,‡ Sebastian Bette,‡ and Melanie Oestreich‡

†*Max Planck Institute for Solid State Research, Heisenbergstrasse 1, D-70569 Stuttgart, Germany, and*
‡*TU Bergakademie Freiberg, Institute of Inorganic Chemistry, Leipziger Strasse 29, D-09595 Freiberg, Germany*

Received March 11, 2010

The metastable phase $9Mg(OH)_2 \cdot MgCl_2 \cdot 4H_2O$ (9-1-4 phase) was found at the extended metastable isotherm of $Mg(OH)_2$ in the system $MgO-MgCl_2-H_2O$ at 120 °C and occurs as intermediate binder phase during setting of magnesia cement due to temperature development of the setting reaction. The crystal structure of the 9-1-4 phase was solved from high resolution laboratory X-ray powder diffraction data in space group *I*2/*m* (*C*2/*m*) ($a = 22.2832(3)$ Å, $b = 3.13501(4)$ Å, $c = 8.1316(2)$ Å, $\beta = 97.753(1)°$, $V = 562.86(2)$ Å^3, and $Z = 1$). Structural and characteristical relations of the phases in the system $MgO-MgCl_2-H_2O$ can be derived, with which the development of the cement or concrete qualities becomes explainable.

Introduction

Basic magnesium salt hydrates form the basis for the use of magnesium oxide as building material. The binder phases are formed by reaction of concentrated magnesium chloride solution with caustic magnesium oxide. This reaction was first observed in 1867 by Stanislas Sorel.[1] From later publications of numerous authors, the general composition: $x Mg(OH)_2 \cdot y MgCl_2 \cdot z H_2O$ of the so-called Sorel cement was established. Since its discovery, the material has been used as floor material, for the production of billiard balls (artificial ivory), and bonding agents in wet stones application. In addition, the material has been used for many years as a barrier construction material in salt formations, since, particularly in the potash mining, the magnesia cement is stable toward salts and their solutions. Within the current concepts[2] of modern waste repositories in salt rocks, among other things as final disposal for radioactive wastes, new requirements are posed regarding the workability of the building material. With the formulation development, the control of the temperature during setting and the guarantee of the desired volume development, the avoidance of cracking and chemical long-term stability (no corrosion by intruding brines due to an equilibrium state) is related. Therefore, phase formation and phase stability under different conditions, such as the influences of temperature, MgO quality, additives, carbon dioxide, and corrosive solutions, need to be known for successful application of this special building material. In particular, temperature-dependent phase formations of magnesium salt hydrates in the primary system $MgO-MgCl_2-H_2O$ are very important, since during the setting procedure temperatures over 120 °C can be reached.

In the literature a lot of phase stoichiometries can be found, of which most remain unconfirmed. The essential discussions refer to the two binder phases, the 3-1-8 phase with the formula $3Mg(OH)_2 \cdot MgCl_2 \cdot 8H_2O$ and the 5-1-8 phase with the formula $5Mg(OH)_2 \cdot MgCl_2 \cdot 8H_2O$. Fundamental and extensive investigations were carried out by Feitknecht,[3−6] Walter-Levy,[7,8] and Bury.[9] The formation conditions regarding the production of magnesia building materials were examined by different authors.[10−17] The crystal structure of the 3-1-8 phase was published in 1953 by De Wolff and Walter-Levy[18]

*To whom correspondence should be addressed. E-mail: r.dinnebier@fkf.mpg.de (R.E.D.); Daniela.Freyer@chemie.tu-freiberg.de (D.F.).

(1) Sorel, S.; Dumas, M. *C. R. Acad. Sci. Paris* **1867**, *65*, 102.
(2) *Radioactive Waste Management - Engineered Barrier Systems* (*EBS*) *in the Safety Case: Design Confirmation and Demonstration*; Workshop Proceedings, Tokyo, Japan, September 12−15, 2006; OECD Publishing: Paris, 2007
(3) Feitknecht, W. *Helv. Chim. Acta* **1926**, *9*, 1018.
(4) Feitknecht, W.; Held, F. *Helv. Acta* **1927**, *10*, 140.
(5) Feitknecht, W.; Held, F. *Helv. Acta* **1930**, *13*, 1380.
(6) Feitknecht, W.; Held, F. *Helv. Acta* **1944**, *27*, 1480.
(7) Walter-Levy, L.; de Wolff, P. M. *C. R. Acad. Sci. Paris* **1949**, *229*, 1077.
(8) Walter-Levy, L.; de Wolff, P. M. *C. R. Acad. Sci. Paris* **1949**, *229*, 1232.
(9) Bury, C. R.; Davies, E. R. H. *J. Chem. Soc.* (*London*) **1932**, 2008.
(10) Newman, E. S.; Gilfrich, J. V.; Wells, L. S. *J. Res. Nat. Bur. Stand.* **1952**, *49*(6), 377.
(11) Harper, F. C. *J. Appl. Chem.* **1967**, *17*(1), 5.
(12) Solovjeva, E. S.; Smirnov, B. I.; Segalova, E. E.; Rebinder, P. A. *Kolloidn. Zh.* **1968**, *30*(5), 754.
(13) Smirnov, B. I.; Solovjeva, E. S.; Segalova, E. E.; Rebinder, P. A. *Kolloidn. Zh.* **1969**, *31*(3), 440.
(14) Beaudoin, J. J.; Ramachandran, V. S. *Cem. Concr. Res.* **1975**, *5*(6), 617.
(15) Sorrell, C. A.; Armstrong, C. R. *J. Am. Ceram. Soc.* **1976**, *59*(1−2), 51.
(16) Matkovic, B.; Popovic, S.; Rogic, V.; Zunic, T. B.; Young, J. F. *J. Am. Ceram. Soc.* **1977**, *60*(11−12), 504.
(17) Urwongse, L.; Sorrell, C. A. *J. Am. Ceram. Soc.* **1980**, *63*(9−10), 501.
(18) de Wolff, P. M.; Walter-Levy, L. *Acta Crystallogr.* **1953**, *6*, 40.

 Published on Web 10/01/2010

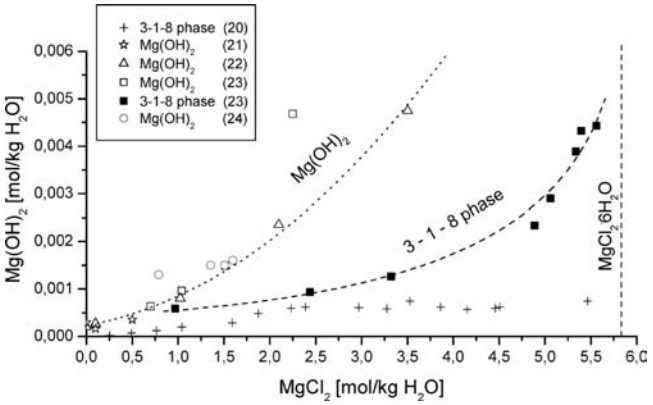

Figure 1. Phase equilibria in the system $MgO-MgCl_2-H_2O$ at 25 °C, literature data.

from powder diffraction data recorded on Guinier-film. Recently, the structure of the 5-1-8 phase was solved from high quality laboratory powder diffraction data by Sugimoto et al.[19] For the evaluation of the chemical long-term stability of a magnesia cement or concrete, the temperature-dependent solubility data of the phases in the system $MgO-MgCl_2-H_2O$ must be known. Only very few thermodynamic data exist for the system at room temperature[20−24] (Figure 1). Thus, in contact with $MgCl_2$ solution (above 1 mol/kg H_2O), the 3-1-8 phase is the thermodynamically stable phase. In the presence of a lower concentration (< about 1 mol of $MgCl_2$/kg of H_2O) the 3-1-8 phase disintegrates into brucite, $Mg(OH)_2$. Data for brucite also exist in the metastable region to about 4 mol of $MgCl_2$/kg of H_2O with higher solubility than for the stable 3-1-8 phase. The 5-1-8 phase, with which the highest concrete strengths are reached, was never found as an equilibrium phase in contact with the solution, and can thus be regarded as metastable phase at ambient temperature.

At 100 and 110 °C, the basic magnesium salt hydrates with the formulas 9-1-5 and 2-1-4 were found in the ternary system by Demediuk et al. in 1955[25] and Walter-Levy and Bianco in 1951.[26,27] In the latter work, the phases 2-1-2 and 3-1-1 also are named.[27] Unfortunately, from these data it is not possible to construct a phase diagram for the system $MgO-MgCl_2-H_2O$ because the general low concentration of $Mg(OH)_2$ in the equilibrium solution is not given.

Because of the difficulties to grow single crystals of sufficient size and quality for single crystal analysis for all ternary phases in the system $MgO-MgCl_2-H_2O$, the crystal structures of high temperature phases were unknown until now, despite their possible influence on the formation on Sorel concrete. In the course of a general investigation to establish the complete ternary phase diagram of the system $MgO-MgCl_2-H_2O$, experiments to derive the solubility data of these phases and to determine their crystal structures using high resolution laboratory X-ray powder diffraction were carried out. The present work focuses on the characterization of the 9-1-5 phase. In the course of the present investigation, the amount of water molecules found in the crystal structure was four, suggesting a name change to the 9-1-4 phase according to the nomenclature given in the introduction.

Table 1. Crystallographic and Rietveld Refinement Data for the 9-1-4 Phase at Ambient Conditions

compound name	9-1-4
molecular formula	$9Mg(OH)_2 \cdot MgCl_2 \cdot 4H_2O$
sum formula	$Mg_{10}Cl_2O_{22}H_{26}$
formula weight (g/mol)	692.192
space group	$I2/m$ ($C2/m$)
Z	1
a/Å	22.2832(3)
b/Å	3.13501(4)
c/Å	8.1316(2)
β/°	97.753(1)
V/Å^3	562.86(2)
temperature (K)	293
ρ (calc)/g cm^{-3}	2.041
wavelength (Å)	1.5406
R-exp (%)[a]	1.76
R-p (%)[a]	2.89
R-wp (%)[a]	3.70
R-F^2 (%)[a]	2.44
starting angle (° 2θ)	6
final angle (° 2θ)	125
step width (° 2θ)	0.009
time/scan (h)	27
no. of variables	51

[a] R-exp, R-p, R-wp, and R-F^2 as defined in TOPAS (Bruker AXS).

Experimental Section

Phase Preparation and Analysis of the System $MgO-MgCl_2-H_2O$ at 120 °C. For determination of the phase equilibria in the system $MgO-MgCl_2-H_2O$ at 120 °C the following reactants were used: magnesium oxide of the company Magnesia with the number M2923, highly reactive (a 50-times higher hydroxide supersaturation is reached during conversion in the solution compared to the equilibrium state at ambient temperature, caused by burning temperature and particle size), and magnesium chloride solution at different concentrations prepared by dissolution of bischofite, $MgCl_2 \cdot 6\,H_2O$ (Fluka, p.a.) in deionized water. The reactants were placed in Teflon cups with a volume of 30 mL situated in TiPd autoclaves. The autoclaves were rotated around their own axis with alternating directions in a metal-block thermostat at constant temperature of 120 ± 0.5 °C for 11−19 days to reach the equilibrium state. Because of the special construction of the autoclaves, the subsequent separation of the solid phase from the solution took place after crossover from the thermostat in a special high temperature centrifuge at 120 ± 1 °C. The entire equipment is described in detail by Freyer et al.[28] Afterward, the autoclaves were cooled down and opened for sampling of the separated phases. The Mg^{2+} concentrations of the solutions were determined by complexometric titration, 0.05 m EDTA (Indicator: Erio T) with an uncertainty of ±1%. By potentiometric titration with 0.1 m $AgNO_3$ the chloride content was quantified with an uncertainty of ±0.1%. In the case of the very low hydroxide concentrations, an appropriate part of the solution was directly, without further dilution, analyzed by acid back-titration. A defined volume of 0.1 m chloride acid was added to the solution sample. For determination of the not neutralized remaining acid, 0.1 m sodium hydroxide solution was used (indicator: phenolphthalein). The uncertainty can be estimated as within ±1%. The solid phases were identified by X-ray powder diffraction in Bragg−Brentano geometry (D5000, Bruker).

(19) Sugimoto, K.; Dinnebier, R. E.; Schlecht, Th. *Acta Crystallogr.* **2007**, *B63*, 805.
(20) Robinson, W. O.; Waggaman, W. H. *J. Phys. Chem.* **1909**, *13*, 673.
(21) Gjaldbaek, J. K. *Z. Anorg. Allg. Chem.* **1941**, *144*, 269.
(22) D'Ans, J.; Katz, W. *Kali Steinsalz* **1941**, *35*, 37.
(23) D'Ans, J.; Busse, W.; Freund, H.-E. *Kali Steinsalz* **1955**, *8*, 3.
(24) Mazuranic, C.; Bilinski, H.; Matkovic, B. *J. Am. Ceram. Soc.* **1982**, *65*(10), 523.
(25) Demediuk, Th.; Cole, W. F.; Hueber, H. V. *Aust. J. Chem.* **1955**, *8*, 215.
(26) Walter-Levy, L.; Bianco, Y. *C. R. Acad. Sci.* (*Paris*) **1951**, *232*, 730.
(27) Bianco, Y. *C. R. Acad. Sci. Paris* **1951**, *232*, 1108.
(28) Freyer, D.; Voigt, W. *Geochim. Cosmochim. Acta* **2004**, *68*, 307.

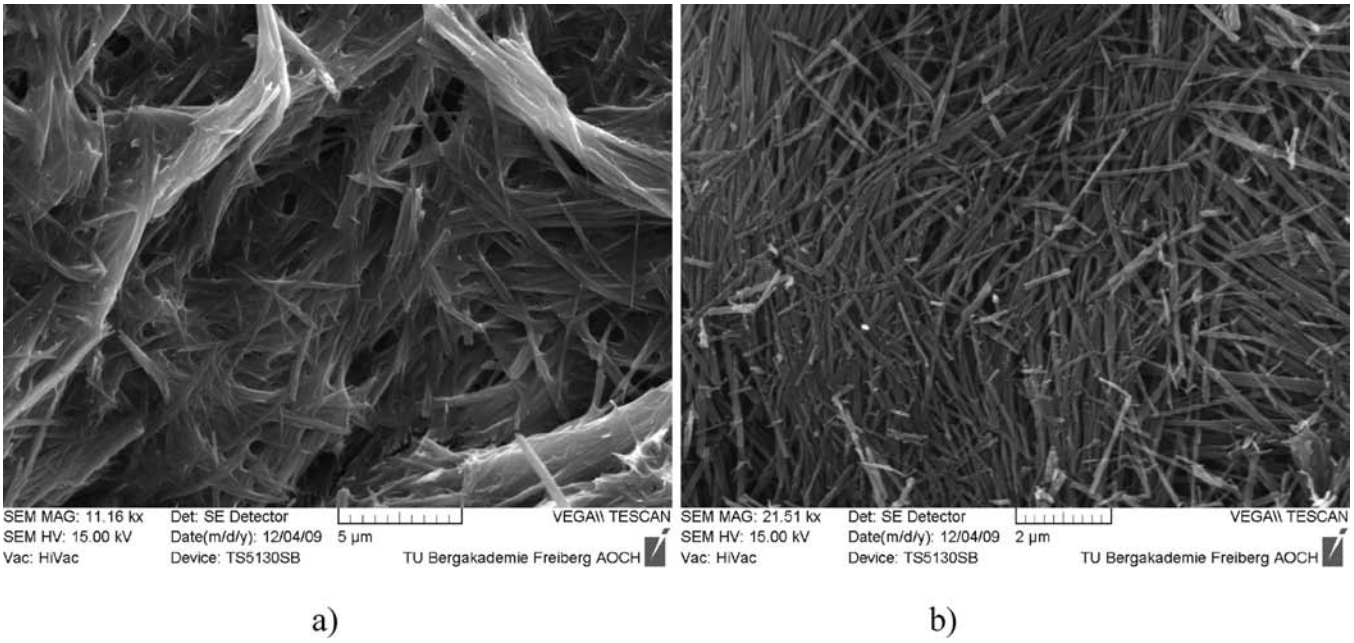

Figure 2. SEM photos of the 9-1-4 phase (a) with adherent mother liquid after shock drying; (b) after washing with water at 0 °C and drying in N_2-stream at 18 °C.

The metastable high temperature phase 9-1-4 (identified by the reference pattern, PDF 07-0409: $Mg_{10}(OH)_{18}Cl_2 \cdot 5H_2O$ = 9-1-5,[26]), No. 6 in Table 1, was prepared for high quality laboratory powder diffraction by subsequent washing with deionized water at 0 °C. Thus, the adhering $MgCl_2$ solution was removed from the phase because bischofite crystallized by drying of the samples. Otherwise, the adherent solution accelerated the formation of the 3-1-8 phase (stable at room temperature) by decomposition of the high temperature phase. Figure 2a shows the very fine crystals of the 9-1-4 phase inserted in the mother liquid (shock dried by generation of high vacuum during the gold sputtering procedure for SEM-monitoring), immediately after separation at 120 °C. The crystals, washed at 0 °C and blow-dried in nitrogen stream at 18 °C, are shown in Figure 2b (washing with water at room temperature leads also to very fast decomposition into the 3-1-8 phase; by several washings with ethanol or acetone the mother liquid could not be removed completely).

Laboratory Powder Diffraction. A high resolution X-ray powder diffraction pattern of the 9-1-4 phase was collected at room temperature on a laboratory powder diffractometer (D8, Bruker, CuKα_1 radiation from primary Ge(111)-Johannson-type monochromator; Våntag-1 position sensitve detector (PSD) with an opening angle of 6°) in Debye−Scherrer geometry with the sample sealed in a borosilicate glass capillary of 0.5 mm diameter (Hilgenberg glass No. 50). The sample was spun during measurement for better particle statistics. Data were taken in steps of 0.009° 2Θ at a scanning speed of 7 s/step (26 h total). For structure determination and refinement, the program TOPAS 4.1[29] was used. Indexing of the diffraction data of the phase was performed by iterative use of singular value decomposition as implemented in the program TOPAS,[30] leading to a monoclinic unit cell (Table 1). The most probable space groups could be determined as $I2/m(C2/m)$ (12), or $I2(C2)$ (5) from the observed extinction rules. From volume increments Z was determined to be 1. The peak profile and precise lattice parameters were determined by a Le Bail fit[31] using the fundamental parameter (FP) approach of TOPAS.[32] Because of the geometry of the Våntac-1

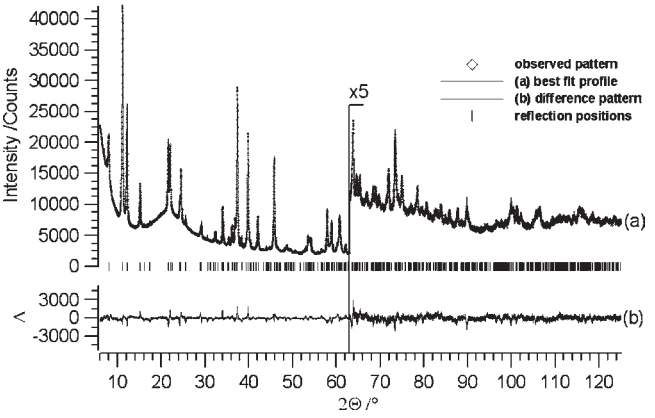

Figure 3. Scattered X-ray intensities of the 9-1-4 phase at ambient conditions as a function of diffraction angle 2θ. The observed pattern (diamonds) measured in Debye−Scherrer geometry, the best Rietveld fit profiles (line), and the difference curve between the observed and the calculated profiles (below) are shown. The high angle part starting at 63° 2θ is enlarged for clarity.

PSD is not fully characterized by FP's, fine-tuning of the available parameters was performed by using refined values of the FP's from a precise measurement of the NIST line profile standard SRM 660a (LaB_6) in a 0.1 mm capillary over the full two theta range of the diffractometer. For the modeling of the background, Chebychev polynomials plus an additional $1/X$ term to describe the air scattering at low angles were employed. In addition, the amorphous hump originating from the glass capillary was successfully modeled by a broad Lorentzian-shaped peak. The refinement converged quickly.

Structure determination of the 9-1-4 phase was performed in space groups $I2/m$ and $I2$ by the method of Charge Flipping[33] supported by the inclusion of the tangent formula[34] as implemented in TOPAS.[35] The positions of all atoms were found in less than a minute using a standard personal computer. By visual

(29) *TOPAS*, version 4.1; Bruker AXS: Madison, WI, 2007
(30) Coelho, A. A. *J. Appl. Crystallogr.* **2003**, *36*, 86.
(31) Le Bail, A.; Duroy, H.; Fourquet, J. L. *Mater. Res. Bull.* **1988**, *23*, 447.
(32) Coelho, A. A. *J. Appl. Crystallogr.* **2000**, *33*, 899.
(33) Oszlányi, G.; Süto, A. *Acta Crystallogr.* **2004**, *A60*, 134.
(34) Karle, J.; Hauptman, H. *Acta Crystallogr.* **1956**, *9*, 635.
(35) Coelho, A. A. *Acta Crystallogr.* **2007**, *A36*, 400.

Table 2. Atomic Coordinates of the 9-1-4 Phase at Ambient Conditions

atom	Wyck.	site	S.O.F.	*x*/*a*	*y*/*b*	*z*/*c*	*U* [Å^2]
Mg1	4i	m		0.5742(1)	1/2	0.2941(3)	1.42(4)
MG2	4i	m		0.3102(1)	0	0.7266(4)	1.42(4)
MG3	2c	2/m		1/2	0	0	1.42(4)
O4	4i	m		0.8424(2)	0	0.0955(5)	0.84(4)
O5	4i	m		0.2187(2)	0	0.6244(5)	0.84(4)
O6	4i	m		0.5186(2)	1/2	0.8370(4)	0.84(4)
O7	4i	m		0.5939(2)	0	0.1300(4)	0.84(4)
O8	4i	m		0.9482(2)	1/2	0.0406(5)	0.84(4)
Cl9	4i	m	0.543(3)	0.3525(2)	0	0.2323(4)	2.5(1)
O10	4i	m	0.592(5)	0.6610(3)	1/2	0.7583(9)	2.5(1)

Table 3. Selected Bond Distances (Å) and Angles (°) of the 9-1-4 Phase at Ambient Conditions

Mg(1)−O	1.952(4) (1x)
	2.142(3) (2x)
	2.167(3) (2x)
	2.193(4) (1x)
Mg(2)−O	2.078(3) (2x)
	2.095(5) (1x)
	2.133(4) (2x)
	2.294(4) (1x)
Mg(3)−O	2.129(2) (3x)
	2.213(4) (3x)
Mg(1)−Mg(2)	3.041(4)
Mg(1)−Mg(1)	3.135(4)
Mg(1)−Mg(3)	3.137(2)
O−O (min)	2.795(6)
Cl−Cl (min)	3.135(1)
O−Mg(1)−O	86.6(1)−94.1(2), 178.5(2)
O−Mg(2)−O	82.8(2)−100.5(2), 172.9(2), 176.1(1)
O−Mg(3)−O	87.3(1)−92.7(1), 180.0

inspection, falsely assigned atom types were detected and corrected. For the final Rietveld refinement,[36] all profile and lattice parameters were released and all atomic positions were subjected to free unconstrained refinement (Figure 3). Refinements in space groups *I*2/*m* and *I*2 converged to identical crystal structures and agreement factors, thus confirming centrosymmetric *I*2/*m* as the correct space group. Final agreement factors (*R*-values) are listed in Table 1. The atomic coordinates are given in Table 2, and a selection of intramolecular distances and angles is given in Table 3. The crystallographic data have been deposited at ICSD under CSD-No. 421571.

Results and Discussion

Solubility Data of the System MgO−$MgCl_2$−H_2O at 120 °C. Compositions of the equilibrium solutions with associated solid phases at T = 120 °C are listed in Table 4. These solubility data are plotted together with the literature data at ambient temperature in Figure 4. At T = 120 °C, the 3-1-8 phase does not exist any longer in the system. Instead, the phases 2-1-4, identified by PDF 00-012-0116,[37] and 2-1-2, identified by PDF 00-012-0133,[37] were found with slightly increased solubilities as compared to that at 25 °C. The 2-1-4 phase is replaced by the 2-1-2 phase above a solution concentration of about 7 mol of $MgCl_2$/kg of H_2O. Our experiments ended at 8 mol of $MgCl_2$/kg of H_2O. With higher concentrations, at 9.2 mol/kg H_2O, magnesium chloride tetrahydrate, $MgCl_2 \cdot 4H_2O$, occurs at 120 °C.[38] At low magnesium chloride concentrations brucite, $Mg(OH)_2$, is existent and can still be isolated from a 3 *m* $MgCl_2$-solution as pure phase. On the extended solubility curve of brucite, a change of the solid phase occurs: brucite is replaced by the 9-1-4 phase (PDF: 00-007-0420 as 9-1-5 phase) at about 4 mol of $MgCl_2$/kg of H_2O and is found in 5 *m* solution as pure phase at the same time with the highest corresponding hydroxide concentration found in the system (0.059 mol of $Mg(OH)_2$/kg of H_2O). Above 5 *m* magnesium chloride solution the phases, 2-1-4 and 2-1-2, with considerably lower solubility are formed. Below 5 *m* magnesium chloride solutions at well extended reaction times up to 20 days, the formation of the these phases could not be achieved so far. Therefore, only an extrapolation from the 2-1-4/2 values to the brucite isotherm at lower chloride concentration is possible. From the solubility diagram (Figure 4), it can be deduced that in comparison to brucite or to the 9-1-4 phase at the same magnesium chloride solution concentration, the 2-1-4 and the 2-1-2 phases (extrapolated from about 6 *m* to about 2 *m* solution, dottet line) show considerable lower solubilities and are the thermodynamically stable phases. Brucite is metastable from approximately 2 *m* solution up to higher concentrations with transition into the 9-1-4 phase. The data at 25 °C show an analogue situation, whereas brucite (open symbols in Figures 1 and 4) is already metastable above 1 *m* solution relative to the 3-1-8 phase.

Table 4. Solubilities in the System MgO−$MgCl_2$−H_2O at 120 °C

	saturated solution [mol/kg H_2O]		
no.	$MgCl_2$	$Mg(OH)_2$	solid phase
1	2.10	0.00581	$Mg(OH)_2$
2	2.08	0.00571	$Mg(OH)_2$
3	3.07	0.01200	$Mg(OH)_2$
4	4.07	0.03985	$Mg(OH)_2$ + 9-1-4 phase
5	4.07	0.04170	$Mg(OH)_2$ + 9-1-4 phase
6	5.01	0.05891	9-1-4 phase
7	5.00	0.05656	9-1-4 phase
8	5.85	0.00511	2-1-4 phase
9	5.85	0.00634	2-1-4 phase
10	6.73	0.00534	2-1-4 phase
11	6.74	0.00556	2-1-4 phase
12	7.11	0.00478	2-1-2 phase
13	7.23	0.00743	2-1-2 phase
14	7.94	0.00590	2-1-2 phase
15	7.30	0.00539	2-1-2 phase

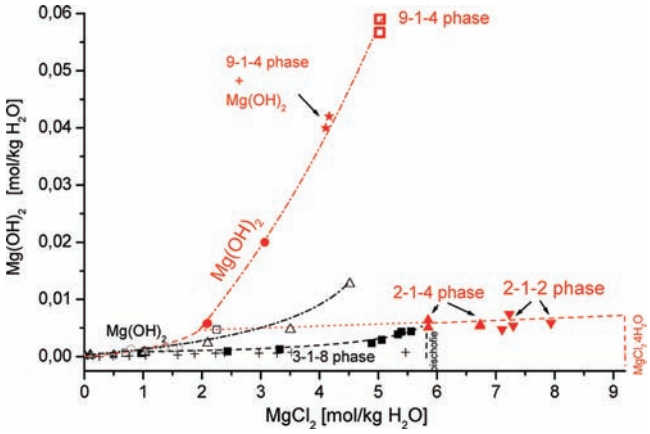

Figure 4. Phase equilibria in the system MgO−$MgCl_2$−H_2O at 120 °C (red) compared to the data at 25 °C from literature (black), as shown in Figure 1.

(36) Rietveld, H. M. *J. Appl. Crystallogr.* **1969**, *2*, 65.
(37) Bianco, Y. *Ann. Chim.* (*Paris*) **1958**, *3*, 370.
(38) Seidel, A.; Linke, W. F. *Solubilities of Inorganic and Metal Organic Compounds*, 4th ed.; American Chemical Society: Washington, DC, 1965, Vol. *2*.

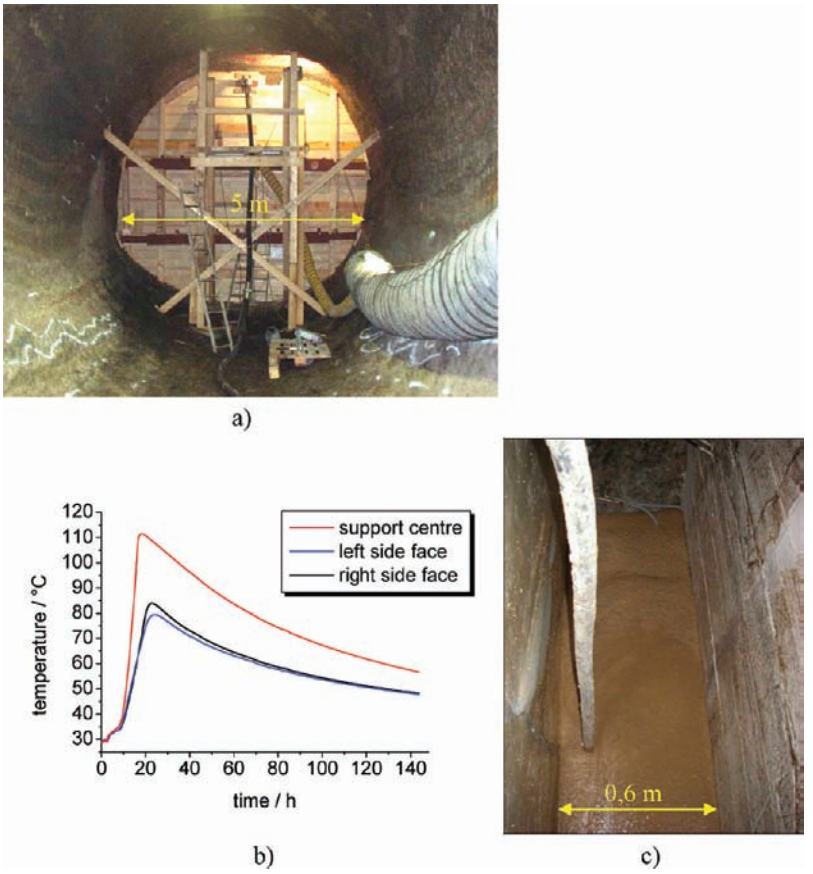

Figure 5. (a) Construction of a magnesia concrete barrier (diameter: 5 m; total length upon completion: 8.4 m) in the potash mining Teutschenthal (Germany) with (b) developing of temperature during setting, monitored in situ at different positions of construction in (c) one concreting step of 5 m × 0.6 m.

Phase Formation during Setting Process. The formation of the Sorel phases in the system $MgO-MgCl_2-H_2O$ is an exothermic reaction, caused by decrease of hydroxide supersaturation developed by mixing of caustic magnesium oxide with concentrated magnesium chloride solutions. All Sorel phases crystallize as fine long needles (example of 9-1-4 phase in Figure 2). A high degree of needle entanglement is reached by fast mass crystallization in the appropriate cement formulations, leading to high strength of the final material.

The chemical inorganic facts regarding phase stability, solubility, and structure presented in this work are the main points with references to application-oriented special conditions. For example, the construction of a magnesia concrete barrier in salt deposits leads to an increase in temperature, as can be seen from the example of the modern potash mining deposit Teutschenthal (Germany). The barrier was constructed by the Institute of Mining, TU Bergakademie Freiberg, within the scope of a current common integrated research project "Development of a basic concept of long term safety barriers in the soluble salt rock for underground waste deposits". During the construction the temperature was monitored in situ, beginning with dumping the concrete formulation (Figure 5). The later mechanical properties of the concrete and their changes in contact with salt solution are dependent from the way and kind of the binder phase formation and were not understand up to now concerning the chemical processes. Thus, according to the temperature history, appropriate smaller amounts of cement formulations in the

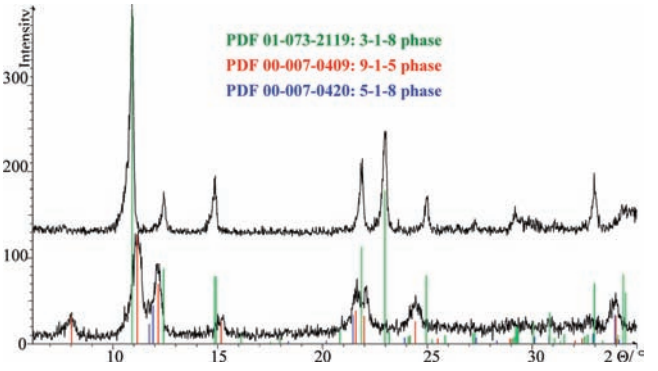

Figure 6. X-ray powder patterns of Sorel cement, 24 h after setting at 80 °C (lower pattern) and at ambient temperature 28 days later (upper pattern) with a 1 kg formulation of the mole ratio $3MgO/1MgCl_2/11H_2O$.

laboratory were kept at 80 °C for 1 and 2 days before cooling down for phase determination. For the experiment, in addition to the magnesia oxide M2923 (Magnesia), the technical MgO of the company Styromag also was used, from which underground constructions in higher dimensions were established. The reactivity of the technical Styromag-MgO is substantially smaller (a 4-times higher hydroxide supersaturation is reached during conversion in the solution as compared to the equilibrium state at ambient temperature) than that of M2923-MgO.

With the cement formulation in moles: $3MgO/1MgCl_2/11H_2O$ (here the $1MgCl_2/11H_2O$ ratio is equivalent to 5 mol of $MgCl_2$/kg of H_2O, an appropriate solution of

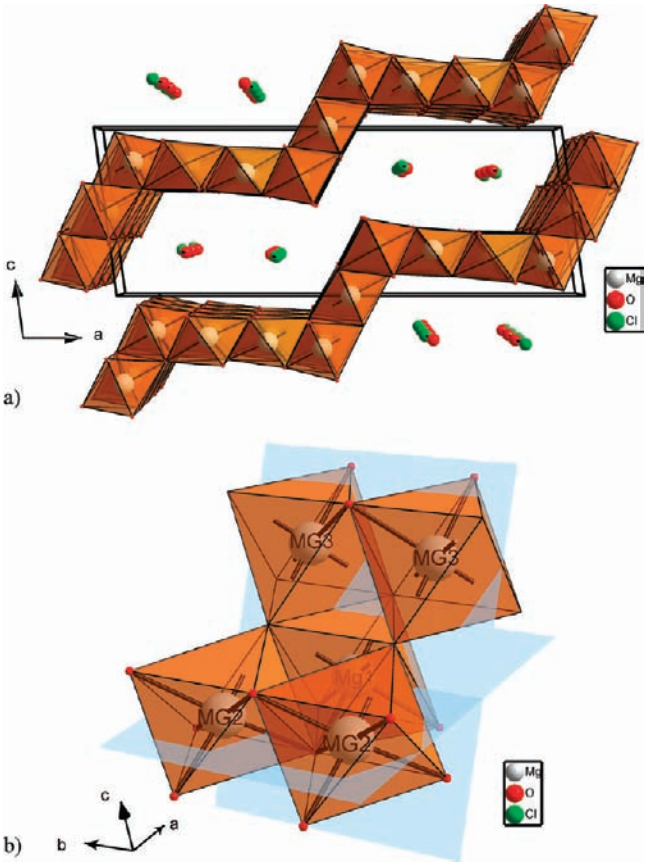

Figure 7. Packing diagram of the 9-1-4 phase at ambient conditions in a view (a) along the *b*-axis and (b) detail showing the dihedral angle of 115.6(1)° between the two molecular planes in the corroborated layers.

bischofite was used) the long-term stable binder phase 3-1-8 forms. In both cases, during the setting process at 80 °C the metastable phase 9-1-4 occurs as the first crystalline phase from these two caustic magnesium oxides types with the 5 *m* magnesium chloride solution according to the formulation. The phase can still be found in the material after cooling down from 80 °C to room temperature (Figure 6). After time and accelerated in contact with pore solution the transformation toward the 3-1-8 phase takes place according to the following equations:

$$3MgO + MgCl_2 + 11H_2O \rightarrow 1/3[9Mg(OH)_2 \cdot MgCl_2 \cdot 4H_2O]$$

$$+ 2/3MgCl_2 + 20/3H_2O \rightarrow 3Mg(OH)_2 \cdot 1MgCl_2 \cdot 8H_2O$$

Additionally, the formation of the intermediate 5-1-8 phase can be observed as a minor phase from X-ray powder diffraction patterns. The 3-1-8 phase occurs after some days of setting as the only binder phase in the material (Figure 6).

Crystal Structure of the 9-1-4 Phase. According to the structure determination from powder diffraction data, a formula unit of this Sorel phase contains only four instead of the originally expected five water molecules.[24−26] No additional electron density could be located. Therefore, the correct chemical composition is more likely described as 9-1-4 instead of 9-1-5. Although unlikely, it cannot be completely ruled out by crystallographic methods that additional disseminated water is present in the crystal structure.

The crystal structure of the 9-1-4 phase consists of corrugated layers of edge- and corner linked distorted MgO_6 octahedra perpendicular to [$\bar{1}$01] direction which

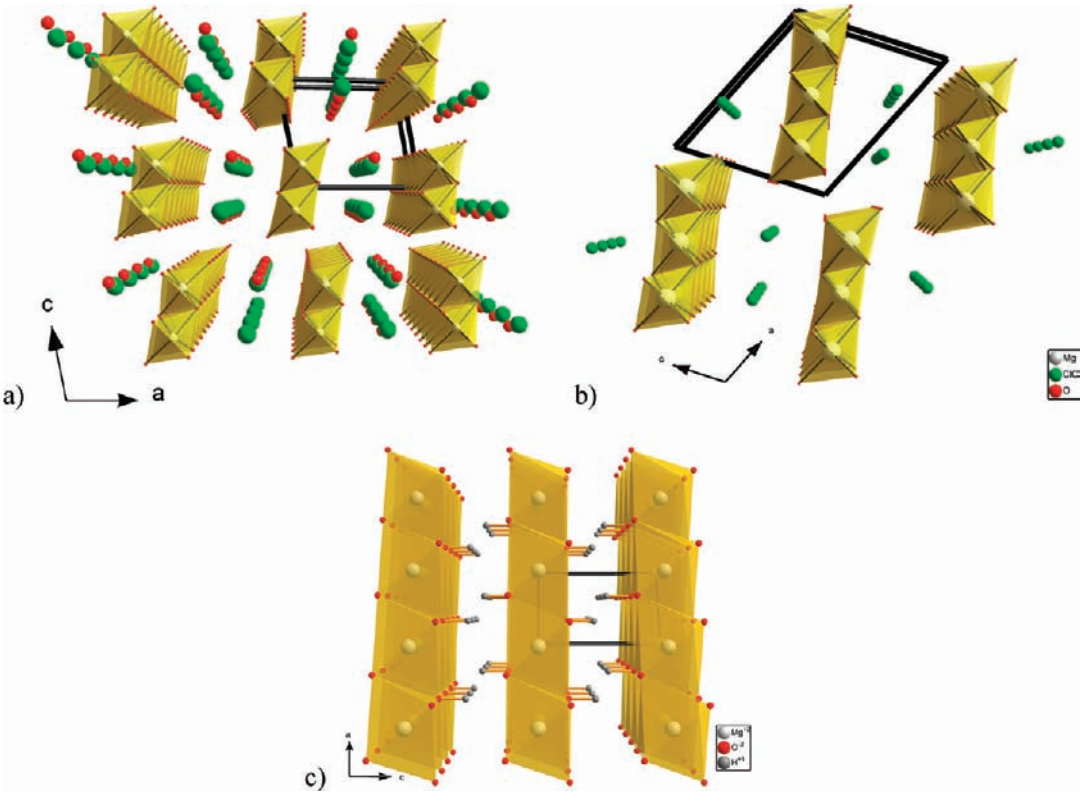

Figure 8. Packing diagrams of the (a) 3-1-8 phase, (b) 5-1-8 phase, and (c) $Mg(OH)_2$ at ambient conditions in perspective views along the *b*-axis.

are separated by interstitial one-dimensional zigzag chains of disordered Cl^- ions and H_2O molecules (Figure 7a). Within the corrugated layers, the angle between the planes is 115.6(1)° (Figure 7b). Each MgO_6 octahedron is connected to eight neighboring octahedra, to six by corner-sharing, and to two by edge sharing. The occupancy factors of the interstitial chlorine and oxygen atoms refined to 0.54 and 0.59, respectively, indicating the presence of Cl^- ions and H_2O molecules with half occupancy. In a fully occupied ordered crystal structure, the Cl^- ions and H_2O molecules would be arranged in an alternating zigzag fashion with a distance of only 1.6 Å which apparently is too short. Since with half occupancy, on average, every second position is occupied, neighboring chains are arbitrarily shifted by 1/2 of the length of the *b*-axis. The crystal structure is stabilized by H-bonds formed between the OH, OH_2 groups of the layers, and the interstitial Cl^-/H_2O.

In comparison to the other phases with known crystal structure in the system $MgO-MgCl_2-H_2O$, the 3-1-8 phase,[18] and the 5-1-8 phase,[19] a clear trend in the condensation of the MgO_6 octahedra with respect to the $Mg(OH)_2$ content is visible. In the crystal structure of the triclinic 3-1-8 phase, *double* chains of $Mg(OH)_4(OH_2)_2$ octahedra run along the *b*-axis, parallel to alternately ordered chains of intercalating chlorine atoms and water molecules (Figure 8a). The crystal structure of the 5-1-8 phase consists of infinite *triple* chains of MgO_6 octahedra running along the *b*-axis and intercalated disordered chlorine ions and water molecules (Figure 8b). Consequently, in the 9-1-4 phase, the infinite *triple* chains of the MgO_6 octahedra are linked by *double* chains of the MgO_6 octahedra. With respect to the crystal structure of brucite, $Mg(OH)_2$ (Figure 8c) with parallel stacked layers of corner linked MgO_6 octahedra which is formed always from caustic MgO in water, the presence of appropriate chloride ion concentrations seems to open the layer sequence by intrusion of chloride ions and water molecules, thus forming the above-mentioned corrugated layers of the 9-1-4 phase.

Conclusion

Solubility data in the system $MgO-MgCl_2-H_2O$ at 120 °C were generated. The stable phases are $Mg(OH)_2$, 2-1-4 phase, 2-1-2 phase, and $MgCl_2 \cdot 4H_2O$. The metastable phase 9-1-4 was found at the extended metastable isotherm of $Mg(OH)_2$. The crystal structure of the 9-1-4 phase could be solved from high resolution X-ray laboratory powder diffraction data employing the methods of charge flipping and Rietveld refinement. The relation between the crystal structures of the 3-1-8, 5-1-8, and the 9-1-4 phase as well as the 9-1-4 phase and brucite could be established. From these results, the phase formations in relation to the characteristic development of Sorel cement can be understood in more detail. According to the solubility data at 120 °C, the 9-1-4 phase occurs metastably analogous to the 5-1-8 phase at 25 °C.[39] The formation of the stable phases 3-1-8 at 25 °C or 2-1-4 at high temperature seems to be inhibited. Similarly, the formation of the 9-1-4 phase during the setting process of the magnesia cement formulation can be observed. The phase is formed during evolved temperatures and their slow slope in the field above 80 °C. According to the formulation adjustment the primarily crystallized 9-1-4 phase transforms into the stable 3-1-8 phase in presence of the remaining pore solution after cooling down. Thus, the early strength of the magnesia concrete seems to be correlated with the crystallization of the 9-1-4 phase, while the (increased) final strength which is reached in course of weeks until months goes along with a slow conversion into the 3-1-8 phase with a more reorganized structure with respect to the "initial phases" $Mg(OH)_2$ and 9-1-4 phase.

Acknowledgment. The authors are grateful for the financial support provided by the Bundesministerium für Bildung und Forschung (BMBF), the company GTS Grube Teutschenthal (stowing mine), and the Fonds der Chemischen Industrie (FCI).

Supporting Information Available: Listing of the crystallographic information files (CIF) of the 9-1-4 phase. This material is available free of charge via the Internet at http://pubs.acs.org.

(39) Freyer, D.; Voigt, W. *GDCh Monogr.* **2009**, *41*, 67.